July 2018

State Observer for Optimal Control using White-box Building Models

Iago Cupeiro Figueroa
KU Leuven, Belgium; EnergyVille, Belgium, iago.cupeirofigueroa@kuleuven.be

Ján Drgoňa
KU Leuven, Belgium, jan.drgona@kuleuven.be

Mohammad Abdollahpouri
Chalmers University of Technology, Sweden, mohammad.abdollahpouri@chalmers.se

Damien Picard
KU Leuven, Belgium, damien.picard@kuleuven.be

Lieve Helsen
KU Leuven, Belgium; EnergyVille, Belgium, lieve.helsen@kuleuven.be

State observers for optimal control using white-box building models

Iago Cupeiro Figueroa[1,2*], Ján Drgoňa[1], Mohammad Abdollahpouri[3], Damien Picard[1], Lieve Helsen[1,2]

[1] KU Leuven, Department of Mechanical Engineering, Celestijnenlaan 300 - box 2421, 3001 Leuven, Belgium

[2] EnergyVille, Thor Park 8310, 3600 Genk, Belgium

[3] Chalmers University of Technology, Department of Electrical Engineering, SE-41296, Gothenburg, Sweden

* Corresponding Author

ABSTRACT

In order to improve the energy efficiency of buildings, optimal control strategies, such as model predictive control (MPC), have proven to be potential techniques for intelligent operation of energy systems in buildings. However, in order to perform well, MPC needs an accurate controller model of the building to make correct predictions of the building thermal needs (feedforward) and the algorithm should ideally use measurement data to update the model to the actual state of the building (feedback). In this paper, a white-box approach is used to develop the controller model for an office building, leading to a model with more than 1000 states. As these states are not directly measurable, a state observer needs to be developed. In this paper, we compare three different state estimation techniques commonly applied to optimal control in buildings by applying them on a simulation model of the office building but fed with real measurement data. The considered observers are stationary Kalman Filter, time-varying Kalman Filter, and Moving Horizon Estimation. Summarizing the results, all estimators can achieve low output estimation error, but, in the case of the Kalman filters, the estimated state values are not physical. In the case of MHE, the model firstly had to be reduced to 200 states in order to evade the non-positive definite quadratic formulation present in the model and converge in tractable computation time.

1. INTRODUCTION

The Paris agreements have led to the ambitious objective of limiting the temperature rise below 2°C this century (Rogelj et al. (2016)). From the global status report towards a zero-emission, efficient, and resilient buildings and construction sector (Dean et al. (2016)), some interesting data can be extracted: buildings and construction together account for 36% of global final energy use and 39% of energy-related carbon dioxide (CO_2) emissions when upstream power generation is included. The global buildings sector continues to grow, with total floor area reaching an estimated 235 billion m^2 in 2016. Final energy use by buildings grew from 119 exajoules (EJ) in 2010 to nearly 125 EJ in 2016. Fossil fuel use in buildings remained almost constant since 2010 at roughly 45 EJ. It is clear that the buildings sector should concentrate efforts to achieve the aforementioned objectives.

Intelligent building control is one of the technologies that can contribute significantly to these goals. Traditional building controllers act based on fixed rules. They are not able to provide an efficient control, especially in complex hybrid systems where the degree of freedom to control the building is high. However, over the past decade MPC has gained the attention of the research community due to its optimal behavior properties. MPC is based on an iterative mathematical optimization of an objective using a controller model over a prediction horizon. In some pilot buildings where it has been implemented, MPC has shown savings of 15-30% (De Coninck & Helsen (2016); Váňa et al. (2014); West et al. (2014)). One crucial aspect of MPC is the controller model (Privara et al. (2013)), whose creation is one of the most time-consuming and challenging parts. According to the nature of the model, this can be black-box if it is purely data-driven and no knowledge is required about its physics, white-box when the model takes into account all physical equations and principles that govern the system, and grey-box when a combination of white and black

box is applied. In this work we opted the white-box approach due to its promising high performance if compared to a grey-box approach (Picard et al. (2016)).

At each computation step, the controller states of the model will be re-initialized. A common simplification made in simulation studies is to provide a perfect state update between the simulation and the controller model. However, in the case of white-box models, due to such a detailed description, the number of states of the building can be in the order of thousands. Therefore, it seems unrealistic to provide such a perfect update since in a real building the amount of sensors installed will most likely not be that high. Moreover, there are some states, such as internal temperatures within the walls, that in practice are very difficult to measure. A state estimator or state observer is therefore needed.

Multiple state estimation techniques exist in the literature. For a comprehensive review, the authors refer to Ali et al. (2015). In this work, we apply and compare observers from the family of Bayesian estimators, which rely on probabilistic distributions of process and measurement noise. The use of these estimators is recommended when: (i) full information about the dynamics of the system is available and (ii) some of the parameters of the system are not fully available. The observers are applied to the building envelope, since within the white-box approach the states are found in this sub-component and no states are present in the HVAC. Some examples of Bayesian estimators are: Luenberger Observer, Kalman Filter, Moving Horizon Estimation...

The Kalman Filter has been proven to be an efficient state estimation technique in many engineering applications. It has been without any doubt the most popular state estimation technique in different applications. Its simple and practical algorithm depends on linear state space models, and by proper tuning, its performance is sometimes comparable to sophisticated estimation techniques such as the Moving Horizon Estimation (Rao et al. (2003)), even though inherently a Kalman filter can not deal with constraints in its design. Basically, Kalman Filter is the solution to a least-squared optimization problem (Gelb (1974)).

Moving horizon estimation (MHE) is the solution to a constrained dynamic optimization problem. The MHE problem formulation is an approximation of a full information constrained estimation technique. It considers a fixed number of measurements inside a moving time window and this makes it tractable in practice, which is almost impossible for a full information estimation approach. However, the trade off is that the optimality will be lost. The arrival cost term is typically introduced in the MHE formulation to represent the truncated data (Kühl et al. (2011)). Its improved performance can be explained by: including N samples of measurements in the moving time window, possibility of explicitly utilizing the nonlinear dynamics in an optimization problem and incorporating the physical and logical constraints in a dynamic optimization framework. Constraints on the states and parameters can help the estimation method to improve the quality of estimates, which e.g. further provide a better control performance. Constraints on the unmeasured input and output disturbances are usually used to model truncated normal densities.

In this paper three state estimators are compared by their assesing performance in a simulation case study, using real measurements. The structure of the paper is as follows: Section 2 describes the building and its simulation model used to test the estimators, and how the estimator model is generated. Section 3 describes the implementation of the stationary and of the time-varying Kalman filter, and of the moving horizon estimator. Finally, Section 4 compares the performance of the different estimators. Conclusions are summarized in Section 5.

2. BUILDING MODEL

The proposed methodology is applied to the Infrax office building in Dilbeek, Brussels, shown in Fig. 1. In this section, the relevant aspects of the building and its model are presented.

2.1 Building

The Infrax building has 2232 m^2 of floor space spread over 4 floors. This office building contains open-plan offices, cellular offices and meeting rooms. The U-values for the outer walls and roof are between 0.18-0.25 and 0.14-0.15 W/(m^2.K) respectively. The windows have double glazing with a U-value of 1.0 W/(m^2.K) and g-values between 0.45-0.49. The air-tightness of the building is measured with a n_{50} value of 1.3 ACH. Solar gains can be controlled by means of movable horizontal fin shading on the 3rd and 2nd floors, and fixed horizontal fin shading combined with overhangs on the 1st and ground floors. On the building roof 61 PV-panels of 136 W_p (8.3 kW_p) are installed and connected to the grid.

Figure 1: The Infrax building

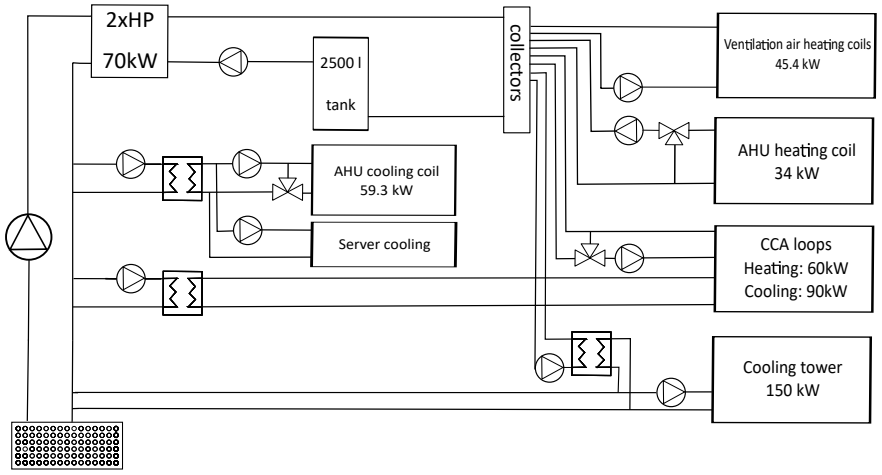

Figure 2: Hydronic schematic of the office building

Fig. 2 shows the hydraulic scheme of the building. Thermal energy is produced by means of 2 geothermal heat pumps of 70 kW_{th} each. The source-side of the heat pumps is connected to a geothermal borefield that is composed of 38 vertical double-U boreholes of 94 m each. The sink-side of the heat pumps is connected to a 2500 l water storage tank and to the main collector, where heat is distributed to multiple distribution loops. In an initial stage, the building was designed to store and cool several server units. Consequently, a 150 kW cooling tower is installed on the source-side to relieve the cooling load of the borefield when needed. Due to the low demand of domestic hot water, a small electrical boiler is installed.

The building has a hybrid emission system that is composed of thermal activated building system (TABS) as a hydronic slow-reacting base load system and of an air handling unit (AHU) that can heat or cool as an air-based, fast-reacting secondary system. The AHU has a nominal supply volumetric flow rate of 10000 m^3/h and a nominal extraction volumetric flow rate of 8850 m^3/h. The AHU is equipped with heating and cooling coils of 34 kW and 59.3 kW respectively, and a heat recovery wheel placed between these coils. The air is distributed over the zones of the building, of which some are equipped with Variable Air Volume (VAV) boxes. Air can be re-heated if needed by using heating coils inside the ducts.

For heating, the aforementioned collector distributes the thermal energy to 4 different heating loops: to the VAV heating coils in the air distribution system (45.4 kW), to the heating coil of the AHU (34 kW), to the TABS system (60 kW) and to the cooling tower (150 kW) in case of dissipation. For cooling, the source side is connected through counterflow plate heat exchangers to the TABS system (90 kW), and to the cooling coil of the AHU and to the server units (106 kW).

2.2 Building model

A white-box model of the building including the building envelope, the HVAC system, and the occupancy has been developed using the Modelica modelling language combined with the `IDEAS` (Jorissen et al. (2018)) and `Buildings`

(Wetter et al. (2014)) libraries. Technical sheets were used to configure the component model parameters, and schematics determine the component interconnections. The building envelope model is composed of 27 zones, of which 21 are conditioned. The 1st, 2nd and 3rd floors are mainly open offices and separate zones exist for the north and south spaces, the individual meeting rooms and the bathrooms (not conditioned). The ground floor includes individual conference rooms and several facilities (first aid, cafeteria, storage and server rooms...).

The HVAC model includes all important hydraulic components of the building, as illustrated in Fig.n 2, and thus allows to control the model up to a high level of detail. The model includes the pressure drops in the main circuits to correctly model the pressure driven flows and to compute the electrical power used by the circulation pump based on similarity laws (Wetter (2013); Wetter et al. (2015)). The valve models compute the pressure drop as a quadratic function of the mass flow rate and the flow-coefficient. This flow-coefficient depends on the control signal and on the valve characteristic (linear, equal-percentage, quick-opening, pressure independent...). The heat pump model consists of a simplified vapor compression cycle with parameters that are calibrated from manufacturer data, as described by (Cimmino & Wetter (2017)). The borefield model allows simulating both short and long term thermal response (Picard & Helsen (2014)).

A rule-based-controller (RBC) was also developed based on the technical description of the building. The first heat pump works with an hysteresis controller to keep the storage tank temperature at 32°C. If the desired temperature is not achieved within 10 minutes, the second heat pump is activated. The cooling tower control is adapted to dissipate heat from the storage tank or to split the load in the borefield in some scenarios. The TABS and the secondary system are operated independently. The TABS has a building climate mode that is computed each day, whereas the secondary system is turned on only during office hours. The supply temperature to the TABS is controlled by means of a mixing three-way valve during heating mode or with the cooling heat exchanger during cooling mode. The supply mass flow rate of the TABS is controlled using four two-way valves, one for each floor. During the neutral mode, water circulates through the TABS in a closed loop. The AHU supply temperature set point is computed using a heating curve that provides a temperature around 18 °C. When additional heating is required, the VAVs are opened to a zone-dependent fixed position and the heating coils supply heat up to a desired supply temperature set-point. When cooling is required the heating coils are not used and the VAVs control the supply air mass flow rate. The building also includes control features for night ventilation and shading.

2.3 Model Linearisation

The Modelica building envelope model, as implemented using the `IDEAS` library, is not directly usable as controller model due to its high complexity. The Modelica reference building model is linearized around a working point in order to obtain a linear SSM. Picard et al. (2015) showed that for a typical Belgium weather (Meteotest, 2009) the linearization error for these equations remains below 1 K. However, the equations for the solar transmission and absorption through the windows are highly non-linear and they should not be linearized. The solar transmission and absorption are instead pre-computed using the `IDEAS` model and they are considered as inputs to the linearized state space model (SSM). For a complete description of the linearization process we refer to Picard et al. (2015).

The obtained discrete time SSM which functions as the estimator model has the following form:

$$x_{k+1} = Ax_k + Bu_k + Ed_k + w_k, \tag{1a}$$

$$y_k = Cx_k + Du_k + v_k, \tag{1b}$$

where x_k, u_k and d_k are states, inputs and disturbances at the *k*-th time step, respectively. Based on the relevant dynamics and associated time constants, a unified sampling frequency $T_s = 15$ min was used as a motivated choice for all investigated model types. Outputs y of the model represent zone temperatures and they are measured by means of temperature sensors. However, this is not the case for the internal states x of the model, which represent temperatures, such as concrete temperatures, that are typically not measurable. The input vector *u* contains the control variables, i.e., the heat flow to each TABS circuit and the heat flow corresponding to the ventilation and VAV input to its room, and the disturbances, i.e., the ambient temperature and the ground temperature, the heat absorbed by and the direct and diffuse solar radiation transmitted by each window, and, finally, the direct, diffuse solar radiation and the environment temperature (i.e. a radiation temperature taking both the environment and the sky temperature into account) per orientation and inclination present in the model. In reality the model is subject to uncertainties, where model uncertainty is represented by the process noise variable w_k and measurement uncertainty is defined by the measurement noise v_k.

3. STATE ESTIMATION

State estimation is typically employed for those systems where measuring all states (or sometimes the parameters of the system) is not possible. The challenge is to solve a problem where the number of known (output and input measurements) is smaller than the number of unknowns (states). In other words, a state estimator is an algorithm that provides an estimate of the internal states of a given real system, from measurements of the inputs and outputs of the real system. The estimation error is defined as the difference between real and estimated states $e_k = x_k - \hat{x}_k$ and is to be minimized during the process of estimation. However, for in practical applications the real states are almost never accessible from the building. Therefore, the output estimation error $ey_k = y_k - \hat{y}_k$ is being used instead for evaluating the estimation performance.Since the obtained building model(eq. (1)) is linearised, we restrict our choice to the following linear estimators: stationary Kalman Filter (SKF), time-varying Kalman Filter (TVKF), and Moving Horizon Estimation (MHE).

3.1 Stationary Kalman Filter

In the case of stationary Kalman Filters (SKF), the estimator gain L is computed by the off-line solution of the discrete Riccati equation given by eq. (2).

$$L = \frac{APC^T + Q}{CPC^T + R + Q} \tag{2}$$

Where P represents estimation error covariance $E(e_k e_k^T)$, Q stands for process noise covariance $E(w_k w_k^T)$, and R for measurement noise covariance $E(v_k v_k^T)$. In this paper MATLAB's `dlqe` function is used to compute L for SKF. In general a Kalman Filter consists of two stages, an update and a prediction phase. The prediction phase eq. (3b) predicts the state at the current time step $k+1$ based on the previous state and the mathematical model of the building. In the update phase eq. (3a) the measurement is used to refine the predicted state estimate from the previous time step by introducing feedback into the system.

$$\hat{x}_{k|k} = \hat{x}_{k|k-1} + L(y_k - C\hat{x}_{k|k-1} - Du_k) \tag{3a}$$

$$\hat{x}_{k+1|k} = A\hat{x}_{k|k} + Bu_k + Ed_k \tag{3b}$$

3.2 Time-varying Kalman Filter

In the case of time-varying Kalman Filters (TVKF) the off-line construction of the estimator gain L is replaced by a recursive on-line computation, defined by the update phase eq. (4) and prediction phase eq. (5).

$$\hat{x}_{k|k} = \hat{x}_{k|k-1} + L_k(y_k - C\hat{x}_{k|k-1} - Du_k) \tag{4a}$$

$$L_k = \frac{P_{k|k-1}C^T}{R_k + CP_{k|k-1}C^T} \tag{4b}$$

$$P_{k|k} = (I - L_k C)P_{k|k-1} \tag{4c}$$

The only difference with SKF eq. (3) is the addition of the recursive updates for the error covariance matrix P via eq. (4c) and eq. (5b) and for the estimator gain L by eq. (4b).

$$\hat{x}_{k+1|k} = A\hat{x}_{k|k} + Bu_k + Ed_k \tag{5a}$$

$$P_{k+1|k} = AP_{k|k}A^T + Q_k \tag{5b}$$

3.3 Moving Horizon Estimation

The moving horizon estimation (MHE) is described as the following optimization problem:

$$\min_{x_{k-N+1},W,V} \; ||x_{k-N+1} - \hat{x}_{k-N+1}||^2_{P^{-1}} + \sum_{i=k-N+1}^{k-1} ||w_i||^2_{Q^{-1}} + \sum_{i=k-N+1}^{k} ||v_i||^2_{R^{-1}} \tag{6a}$$

$$\text{s.t.} \;\; x_{i+1} = Ax_i + Bu_i + Ed_k + w_i, \qquad i \in \mathbb{N}^{k-1}_{k-N+1} \tag{6b}$$

$$y_i = Cx_i + Du_i + v_i, \qquad i \in \mathbb{N}^{k}_{k-N+1} \tag{6c}$$

$$x_i \in \mathcal{X}, \;\; w_i \in \mathcal{W}, \;\; v_i \in \mathcal{V}. \tag{6d}$$

Table 1: Tuning and performance comparison of selected state estimators.

Method	Section	n_x	Q	R	N	ISE	max(ey)	mean(ey)	Sim. time [s]
SKF	3.1	1262	$1e1$	$1e0$	-	16.2	0.62	0.0038	9.9
TVKF	3.2	1262	$1e10$	$1e0$	-	245	1.55	0.0045	819.2
MHE	3.3	200	$1e6$	$1e0$	3	412	2.20	0.0055	1777.7

where x_k, u_k, d_k, w_k and v_k represent the values of states, inputs, disturbances, process and measurement noise respectively, predicted at the *k*-th step of the estimation horizon N. The predictions are obtained from the linear time invariant (LTI) prediction model given by Eqs. (6b) and (6c). Limits on state and noise variables are defined by eq. (6d). The term $||a||_Q^2$ in the objective function represents the weighted squared 2-norm, i.e., $a^T Q a$, with the weighting matrices Q, R, and P given as positive definite diagonal matrices. The first term of the objective function stands for the so called arrival cost, which represents the summarized effect of data from previous timesteps outside the estimation window N. In this case we defined the arrival cost explicitly based on previous state estimates at the (*k-N+1*)-th step.

In general the number of optimization variables include the estimated state over the horizon, the estimated state update error (W) and the estimated measurement error (V). Since for the existing building model the linear SSM is utilized, we can use the commonly known approach of condensing. The first element of the optimized estimated state over the horizon ($\hat{x}_{k-N+1}$) is selected and the current estimated state $\hat{x}_k$ is calculated by integration using W. This technique can efficiently reduces the number of optimization variables and speed up the solver time.

The MHE problem (6) is constructed in the MATLAB environment, using the modeling and optimization toolbox YALMIP (Löfberg, 2004). The objective function (Eq. (6a)) is quadratic and all constraints are linear, therefore problem (6) can be solved as a strictly convex quadratic program (QP). For solving problem (6a) the state of the art optimization solver GUROBI (Gurobi Optimization, 2012) is used.

4. SIMULATION CASE STUDY WITH REAL MEASUREMENTS

4.1 Simulation Setup

The estimator performances are evaluated using four key performance indicators (KPIs): integral square error (ISE) defined by Eq. (7), maximal estimation error max(ey), mean of estimation error mean(ey), and overall simulation time.

$$\text{ISE} = \sum_{k=1}^{N_{\text{sim}}} ey_k \tag{7}$$

N_{sim} stands for the number of simulation steps. Based on the dynamic response of the building model and frequency of the measurement data, the sampling period was chosen equal to $T_s = 480$ s. The state values $x(0)$ are initialized at $20°C$, based on the procedure described in our previous work (Picard et al., 2017). The disturbance vector d is generated from a typical year in Uccle, Belgium (Meteotest, 2009). Based on available measurement data in the real office building, the overall simulation period is chosen to be 14 days. All three state estimators are tuned such that they provide best performance and their tuning parameters are summarized in Tab. 1. The tuning factors used were the process noise covariance Q and the measurement noise covariance R matrices, which are designed as diagonal positive definite matrices. In the case of SKF and TVKF a full order model with 1262 states is used as a prediction model. On the other hand, for MHE a reduced order model (ROM) with 200 states and prediction horizon $N = 3$ is used to reduce the computational burden. Besides, with a full order model (FOM) the MHE was not feasible because the objective function of the resulting quadratic problem was not positive definite. The ROM is obtained as the the best possible linear representation of the original model by using the balanced truncation method, for a detailed description of the model order reduction (MOR) methodology we refer to Picard et al. (2017).

4.2 Measurement Data

The measurement data for this experiment are extracted from the Building Management System (BMS) of the office building for the period 22-02-2018 to 08-03-2018 (14 days). The frequency of the measurement data storage in the database is 480 seconds. The BMS can store up to 175 data points of the building, meaning that not all information is available and a selection of data points has to be made in a pre-processing step. Among other data needed for the sake of maintenance and fault detection, points collected include: TABS 2-way valve positions, mixing 3-way valve positions, temperatures in the hydronic circuit, air supply temperatures, temperatures of the different zones, CO_2 level of the different zones, VAV damper positions, AHU supply and extract fan normalized signals, signals to the hydraulic pumps, climate mode of the building and mass flow and energy use of the calorimeters. Due to a lack of sensors in some of the zones, several data points of the building have to be post-processed to transform them as inputs to the building, according to the given RBC description of the building.

4.3 Results

The estimation profiles of SKF, TVKF and MHE are shown in Fig. 3, Fig. 4, and Fig. 5, respectively. The top figure represents trajectories of measured outputs depicted in solid lines and trajectories estimated outputs shown in dashed lines. The middle figure shows output estimation error profiles, while bottom figure depicts estimated state trajectories. The comparison based on selected KPIs is given in Tab. 1. Fig. 6 compares box plots of estimation errors for each thermal zone. When the one-step ahead output estimation error is considered, all investigated estimators seem to be well designed and tuned as ey remains small for all zones and all estimators and its mean is around zero (see fig. 6). However, the estimated state trajectories show unrealistic values with temperatures between -50 to 40°C. Even though these values lead to a low one-step ahead output estimation error, it is likely that a N-step ahead prediction would show a large error. This analysis is less obvious for MHE as, due to model order reduction, the state values lost their physical meaning.

The reason why the state estimators return unrealistic state values should be further investigated before applying the method in the control of the real building. A possible explanation is that the plant-model mismatch is too high and that only unrealistic state values could be used to mimic the actual system. Furthermore, it should be noted that the state estimator problem is complex as only a limited number of measurement data (19 zone temperatures) is used to estimate a large number of states (1262). Another possible explanation is that the number of measurements are not enough to uniquely estimate all the states.

The computational time of MHE is significantly higher when compared to SKF. Nevertheless, considering that the amount of seconds per time-step for the computation is lower than 1, MHE is feasible for real implementation purposes, where the time-steps can be typically from 15 minutes to 1 hour.

5. CONCLUSIONS

Three state estimation methods have been compared to demonstrate the possibility of a closed loop state feedback control design for buildings. Namely, stationary Kalman filter (SKF), time-varying Kalman filter (TVKF) and moving horizon estimation (MHE) were investigated. A linearized building envelope model was used for prediction of the building thermal behavior. The simulation experiments were conducted using real measurements for the period of 13 days. All investigated estimators present low output one-step ahead estimation error. However, the estimated state values show unrealistic values in the case of SKF and TVKF which can lead to inaccuracy for the N-step ahead predictions necessary in MPC. As MHE uses a reduced order model, this reality check could not be performed for that estimator. The MHE the use of a full order model was not feasible because the objective function of the resulting quadratic problem was not positive definite.

Because the building envelope can be well described by linear model adding non-linearities into the model would increase the computational time without significant improvement in the output estimation error. Hence the usage of the non-linear state estimators for the state estimation of the building envelope does not seem reasonable.

Future work will firstly investigate the cause of the unrealistic state values of the Kalman filters (SKF and TVKF). Secondly, the formulation of MHE should be adapted in order to be able to use full order model.

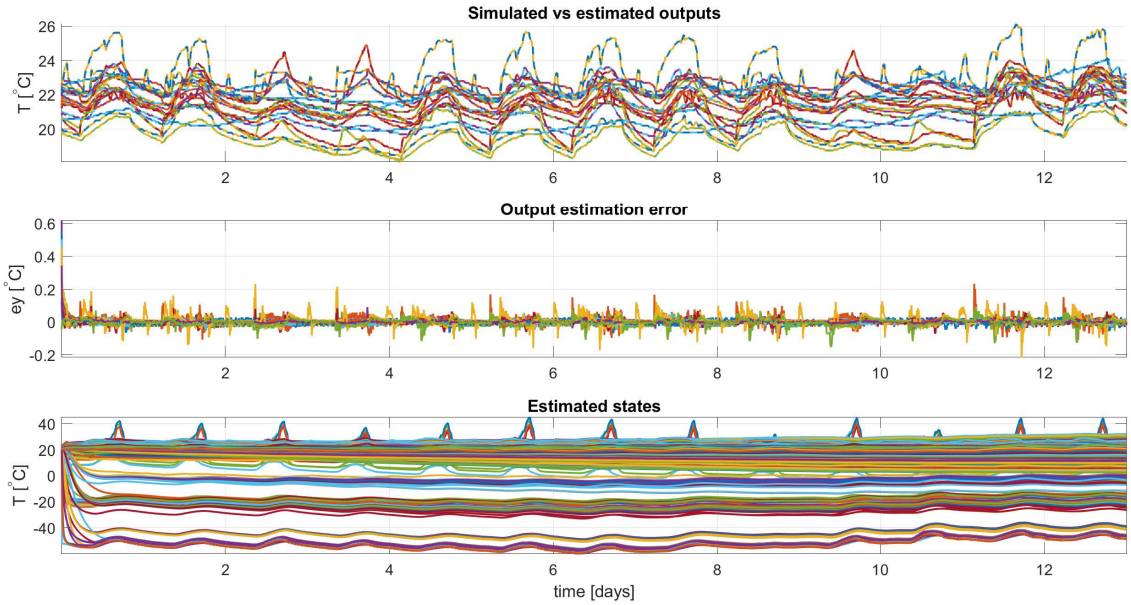

Figure 3: SKF profiles. Top figure: trajectories of measured outputs (solid lines) and estimated outputs (dashed lines). Middle figure: output estimation error profile. Bottom figure: estimated state trajectories.

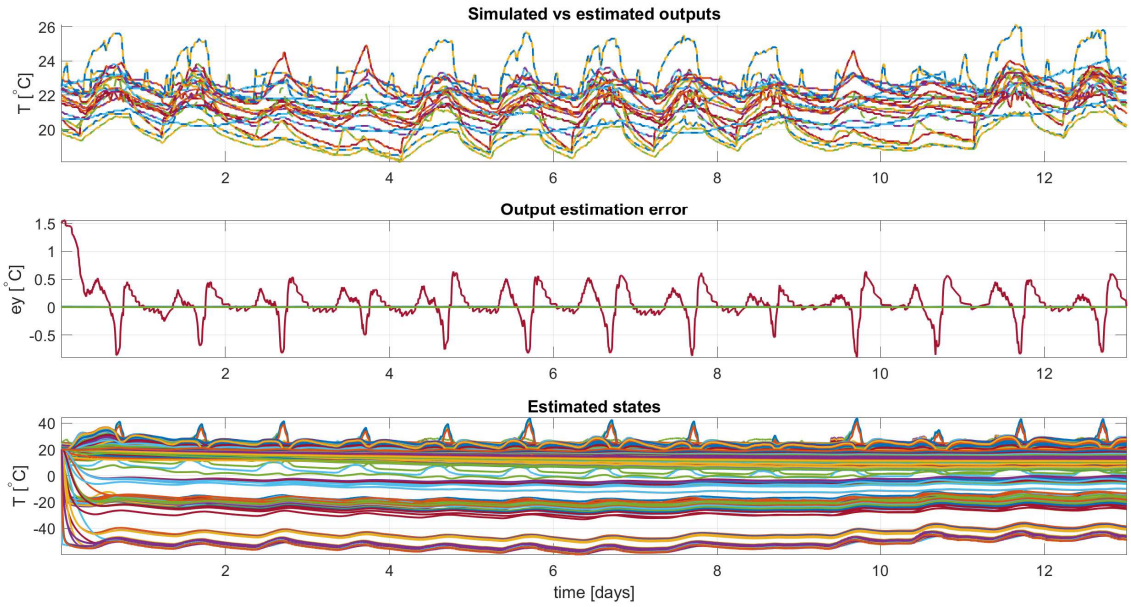

Figure 4: TVKF profiles. Upper figure: trajectories of measured outputs (full lines) and estimated outputs (dashed lines). Middle figure: output estimation error profile. Bottom figure: estimated state trajectories.

ACKNOWLEDGMENT

The authors gratefully acknowledge the funding of their research work by the EU within the H2020-EE-2016-RIA-IA programme for the project 'Model Predictive Control and Innovative System Integration of GEOTABS;-) in Hybrid

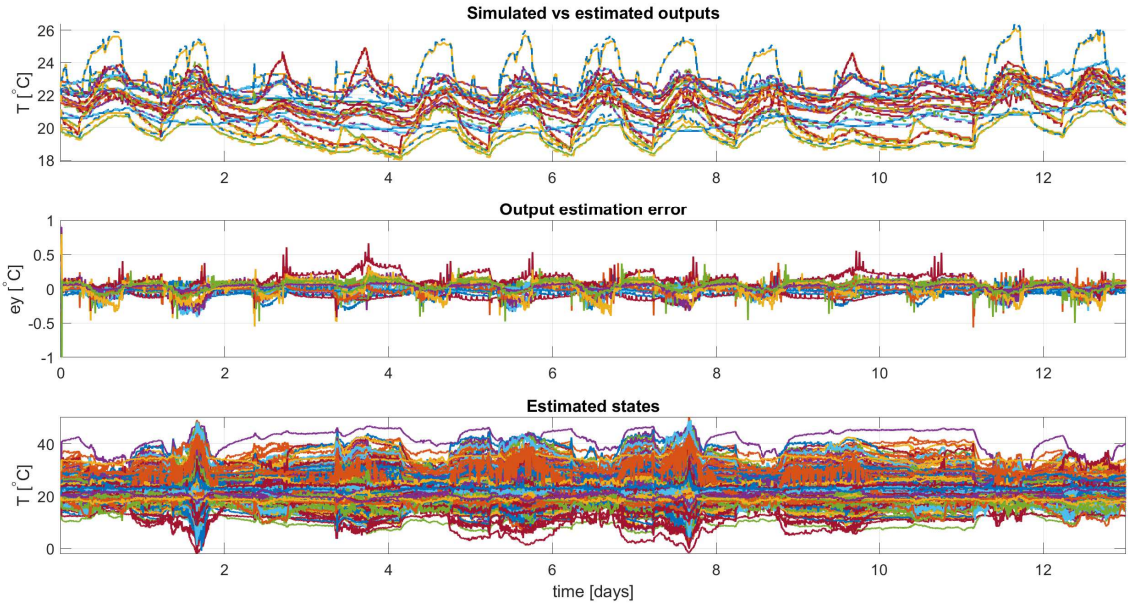

Figure 5: MHE profiles. Upper figure: trajectories of measured outputs (full lines) and estimated outputs (dashed lines). Middle figure: output estimation error profile. Bottom figure: estimated state trajectories.

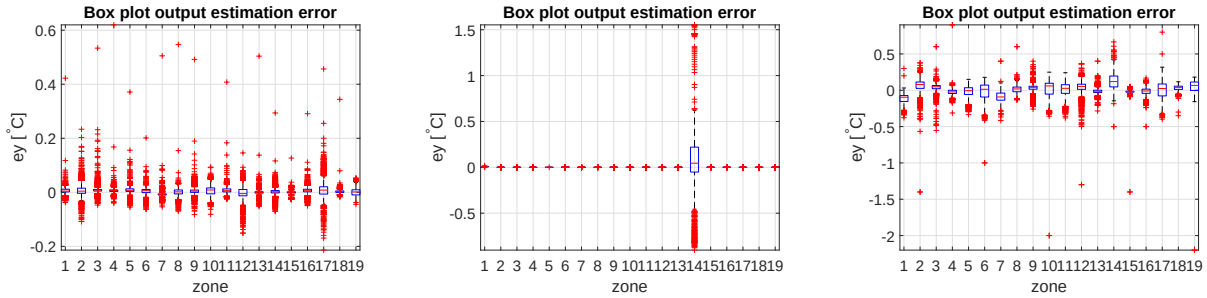

(a) SKF. **(b) TVKF.** **(c) MHE.**

Figure 6: Output estimation error box plots. The centered line gives the median, the box gives the first and third quartiles, the whiskers contain 99.5% of the data, and the crosses are the outliers.

Low Grade Thermal Energy Systems - Hybrid MPC GEOTABS' (grant number 723649 - MPC-; GT), and within the EU-H2020-GEOTECH project 'Geothermal Technology for Economic Cooling and Heating' (grant number 656889 - GEOTECH).

REFERENCES

Ali, J. M., Hoang, N. H., Hussain, M., & Dochain, D. (2015). Review and classification of recent observers applied in chemical process systems. *Computers & Chemical Engineering*, *76*, 27 - 41.

Cimmino, M., & Wetter, M. (2017). Modelling of heat pumps with calibrated parameters based on manufacturer data. In *Proceedings of the 12th International Modelica Conference, Prague, Czech Republic, May 15-17, 2017* (pp. 219–226).

De Coninck, R., & Helsen, L. (2016). Practical implementation and evaluation of model predictive control for an office building in Brussels. *Energy and Buildings*, *111*, 290 - 298.

Dean, B., Dulac, J., Petrichenko, K., & Graham, P. (2016). Towards zero-emission efficient and resilient buildings: Global status report. *International Energy Agency (IEA) for the Global Alliance for Buildings and Construction (GABC), coordinated by the UN Environment Programme*.

Gelb, A. (1974). *Applied optimal estimation*. Cambridge, Massachusetts: The Massachusetts Institute of Technology (MIT) press.

Gurobi Optimization, I. (2012). *Gurobi optimizer reference manual.* "`http://www.gurobi.com`". (Accessed: 2018-04-26)

Jorissen, F., Reynders, G., Baetens, R., Picard, D., Saelens, D., & Helsen, L. (2018). Implementation and Verification of the IDEAS Building Energy Simulation Library. *Journal of Building Performance Simulation*.

Kühl, P., Diehl, M., Kraus, T., Schlöder, J. P., & Bock, H. G. (2011). A real-time algorithm for moving horizon state and parameter estimation. *Computers & Chemical Engineering*, *35*, 71–83.

Löfberg, J. (2004). YALMIP : A Toolbox for Modeling and Optimization in MATLAB. In *Proc. of the CACSD conference.* Taipei, Taiwan. (Available from `http://users.isy.liu.se/johanl/yalmip/`)

Meteotest. (2009). *METEONORM version 6.1 - edition 2009* (Tech. Rep.). Author.

Picard, D., Drgoňa, J., Kvasnica, M., & Helsen, L. (2017). Impact of the controller model complexity on model predictive control performance for buildings. *Energy and Buildings*, *152*, 739 - 751.

Picard, D., & Helsen, L. (2014). A new hybrid model for borefield heat exchangers performance evaluation. *ASHRAE Transactions*, *120*, 9p.

Picard, D., Jorissen, F., & Helsen, L. (2015). Methodology for obtaining linear state space building energy simulation models. In *Proceedings of the 11th international modelica conference* (pp. 51–58). Paris, France.

Picard, D., Sourbron, M., Jorissen, F., Cigler, J., Ferkl, L., Helsen, L., et al. (2016). Comparison of model predictive control performance using grey-box and white box controller models. In *4th International High Performance Buildings Conference* (p. Paper 203). Purdue, West Lafayette.

Privara, S., Cigler, J., Váňa, Z., Oldewurtel, F., Sagerschnig, C., & Žáčeková, E. (2013). Building modeling as a crucial part for building predictive control. *Energy and Buildings*, *56*, 8–22.

Rao, C. V., Rawlings, J. B., & Mayne, D. Q. (2003). Constrained state estimation for nonlinear discrete-time systems: Stability and moving horizon approximations. *IEEE Transactions on Automatic Control*, *48*, 246–258.

Rogelj, J., Den Elzen, M., Höhne, N., Fransen, T., Fekete, H., Winkler, H., ... Meinshausen, M. (2016). Paris Agreement climate proposals need a boost to keep warming well below 2 C. *Nature*, *534*(7609), 631.

Váňa, Z., Cigler, J., Široký, J., Žáčeková, E., & Ferkl, L. (2014). Model-based energy efficient control applied to an office building. *Journal of Process Control*, *24*(6), 790 - 797. (Energy Efficient Buildings Special Issue)

West, S. R., Ward, J. K., & Wall, J. (2014). Trial results from a model predictive control and optimisation system for commercial building HVAC. *Energy and Buildings*, *72*, 271 - 279.

Wetter, M. (2013). Fan and Pump Model that has a Unique Solution for any Boundary Condition and Control Signal. In *13th Conference of International Building Performance Simulation Association* (pp. 3505–3512). Chambéry, France.

Wetter, M., Fuchs, M., Grozman, P., Helsen, L., Jorissen, F., Müller, D., ... Thorade, M. (2015). IEA EBC Annex 60 modelica library-an international collaboration to develop a free open-source model library for buildings and community energy systems. In *Proceedings of Building Simulation 2015.* Hyderabad, India. (December 7-9, 2015)

Wetter, M., Zuo, W., Nouidui, T. S., & Pang, X. (2014). Modelica buildings library. *Journal of Building Performance Simulation*, *7*(4), 253–270.